**Supplemental Figure. 1 *LepR-Cre* mice does not display any abnormal energy homeostasis.**

(**A**) Weekly body weight is shown for *LepR-Cre* mice and control mice fed a NC ($n = 6$, two-way ANOVA with Bonferroni *post hoc* test). (**B**) GTTs

were performed in *LepR-Cre* mice and control mice after a 6 hr fast at 16 weeks of age ($n = 6$, two-way ANOVA with Bonferroni *post hoc* test). (**C**) ITTs

were performed in *LepR-Cre* mice and control mice after a 6 hr fast at 16 weeks of age ($n = 6$, two-way ANOVA with Bonferroni *post hoc* test). (**D** and

E) Adipose tissue weights (**D**) and adipose tissue weights normalized to body weight (**E**) are shown for *LepR-Cre* mice and control mice at 16 weeks of

age ($n = 6$, two-tailed Student's *t*-test). All of the mice used in this study were male.
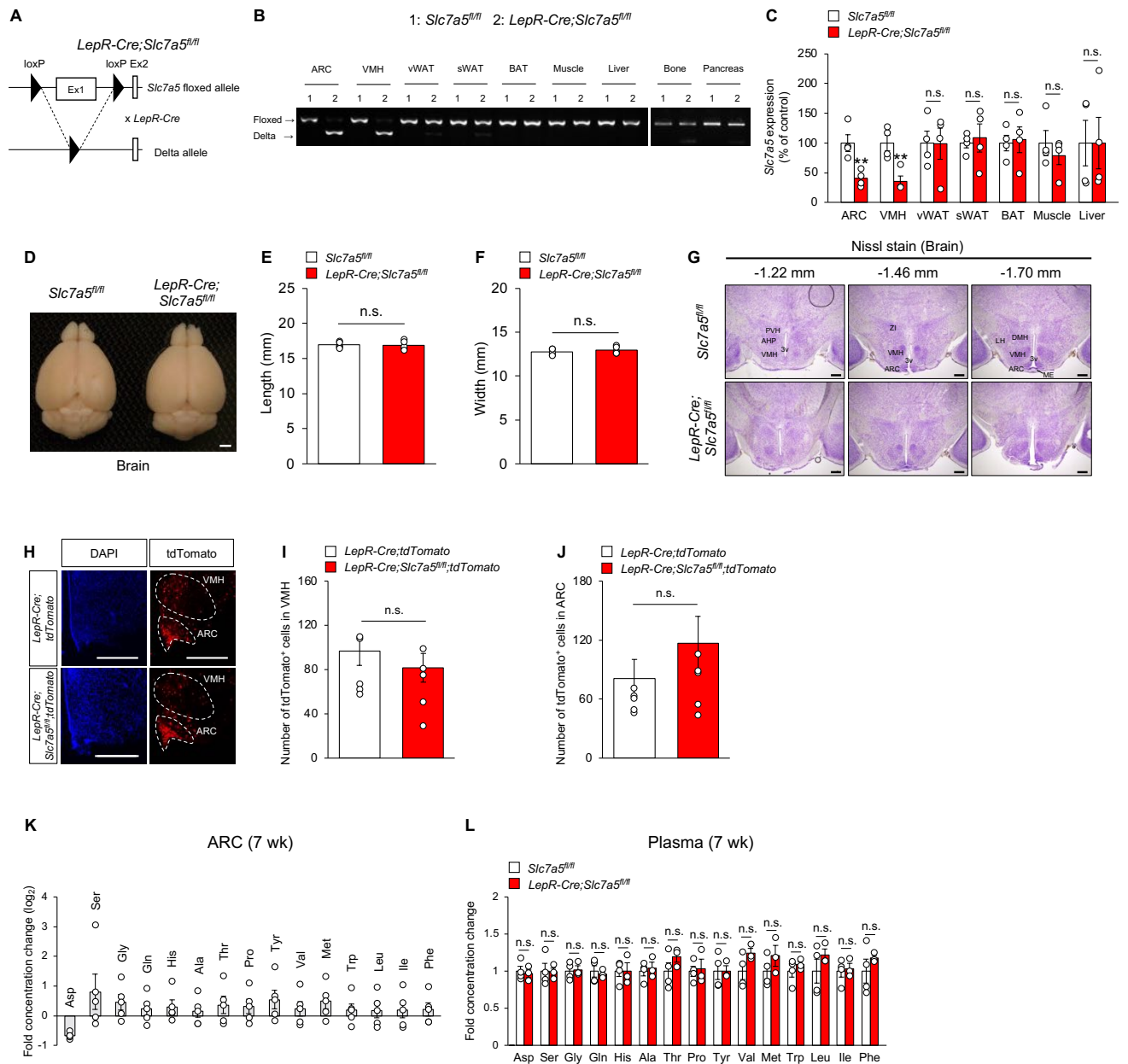
Supplemental Figure. 2 Deletion efficiency and specificity, brain morphology and amino acid levels in *LepR-Cre;Slc7a5fl/fl* mice.

(**A**) Schematic diagram of generating LepR-expressing cell-specific *Slc7a5* knockout mice. (**B**) Deletion efficiency of *Slc7a5* in each region of the hypothalamus and peripheral tissues of *LepR-Cre;Slc7a5fl/fl* mice at the genomic DNA level (floxed: 2004 bp, delta: 253 bp). (**C**) mRNA levels in each region of the hypothalamus and peripheral tissues of *LepR-Cre;Slc7a5fl/fl* mice. ($n = 4$, **$P < 0.01$, two-tailed Student's t-test). (**D-F**) Representative picture (**D**), length (**E**) and width (**F**) of brains are shown for *LepR-Cre;Slc7a5fl/fl* mice and control mice at 7 weeks of age ($n = 5$, two-tailed Student's t-test). Scale bar, 1 mm. (**G**) Nissl stain was performed on the brains of *LepR-Cre;Slc7a5fl/fl* mice at 7 weeks of age. Scale bar, 100 μm. (**H-J**) Representative images of VMH and ARC (**H**) and the number of tdTomato$^+$ neurons in the VMH (**I**) and ARC (**J**) of *LepR-Cre;Slc7a5fl/fl;tdTomato* mice at 7 weeks of age ($n = 7$, two-tailed Student's t-test). Scale bar, 500 μm. (**K**) Log$_2$ ratio of the amino acid levels in ARC between *LepR-Cre;Slc7a5fl/fl* mice and control mice at 7 weeks of age ($n = 5$, two-tailed Student's t-test). (**L**) Amino acid levels in plasma of *LepR-Cre;Slc7a5fl/fl* mice at 7 weeks of age ($n = 3$ or 4, two-tailed Student's t-test). All of the mice used in this study were male.
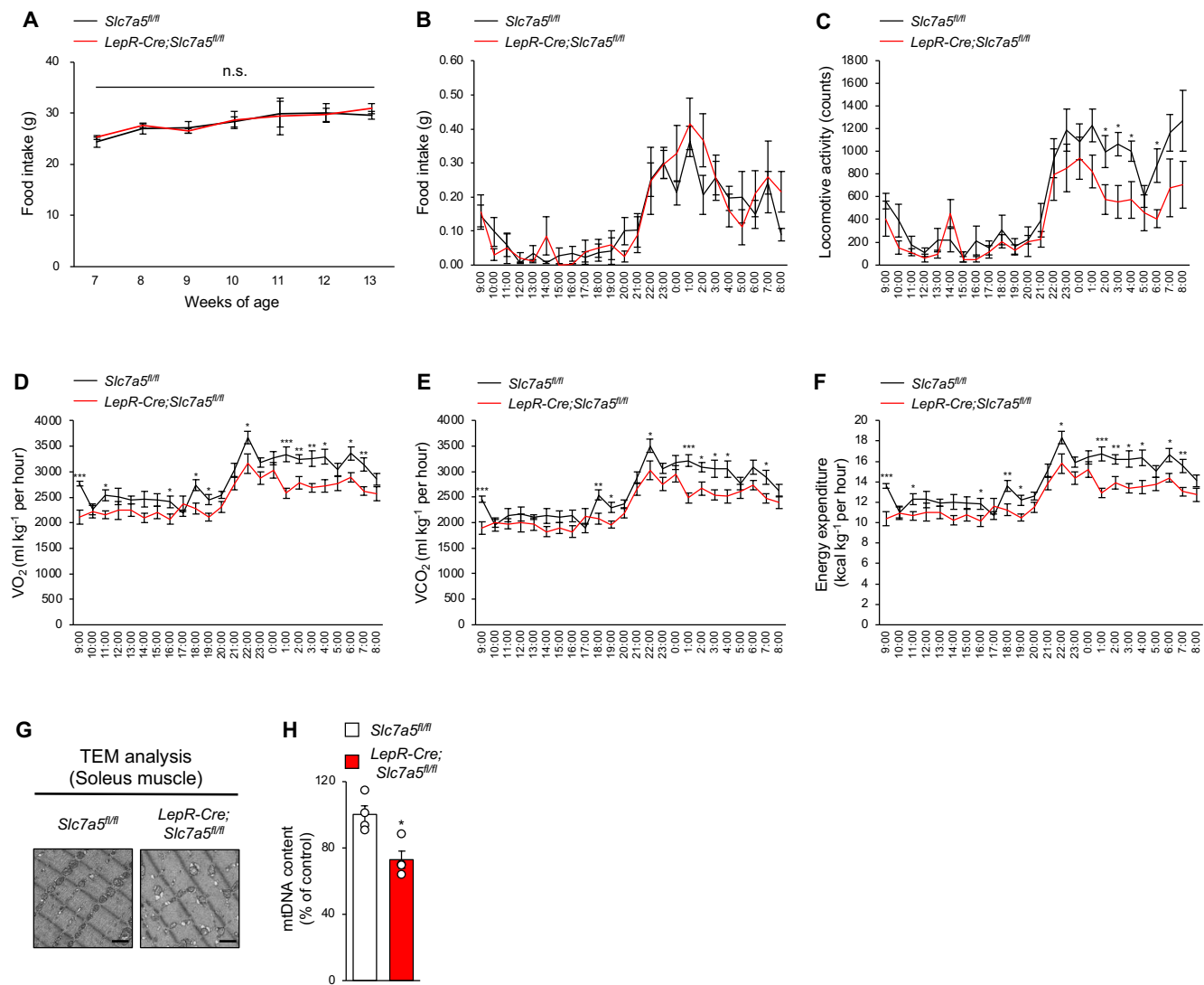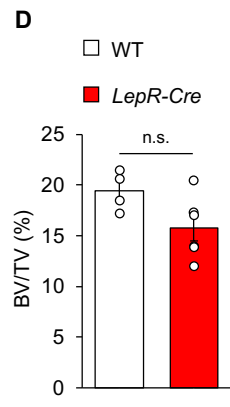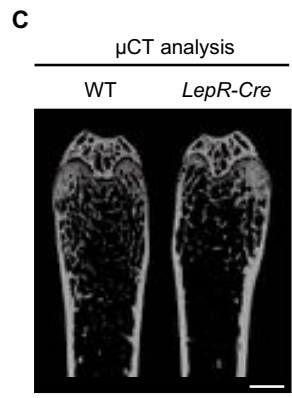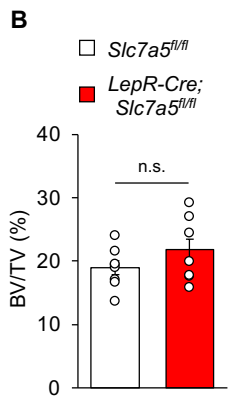
Supplemental Figure. 3 Metabolic parameters and muscle mitochondrial morphology in *LepR-Cre;Slc7a5^{fl/fl}* mice.

(**A**) Weekly food intake is shown for *LepR-Cre;Slc7a5^{fl/fl}* mice and control mice fed a NC (n = 7 or 9, two-way ANOVA with Bonferroni *post hoc* test), (**B-F**) Temporal changes of food intake (**B**), locomotor activity (**C**), O_2 consumption (**D**), CO_2 production (**E**) and energy expenditure (**F**) were measured in singly housed *LepR-Cre;Slc7a5^{fl/fl}* mice and control mice at 22-24 weeks of age (n = 7 or 8, *P < 0.05, **P < 0.01, ***P < 0.001, two-way ANOVA with Bonferroni *post hoc* test). (**G**) TEM analysis was performed on the soleus muscle of *LepR-Cre;Slc7a5^{fl/fl}* mice and control mice at 22-24 weeks of age. Scale bar, 10 µm. (**H**) mtDNA content of soleus muscle was measured in *LepR-Cre;Slc7a5^{fl/fl}* mice and control mice at 22-24 weeks of age (n = 4, *P < 0.05, two-tailed Student's *t*-test). All of the mice used in this study were male.
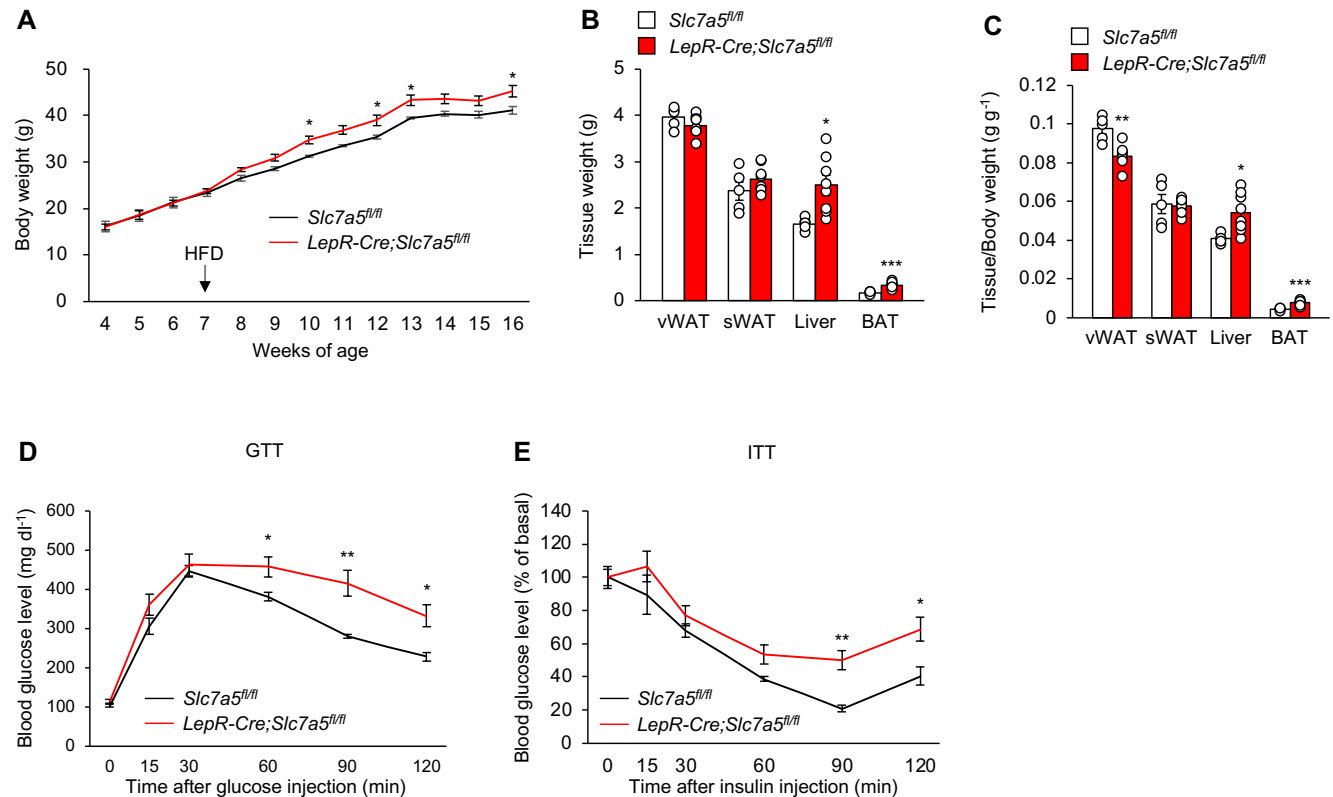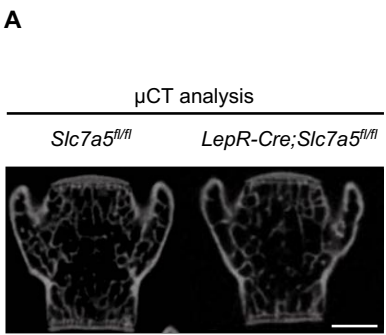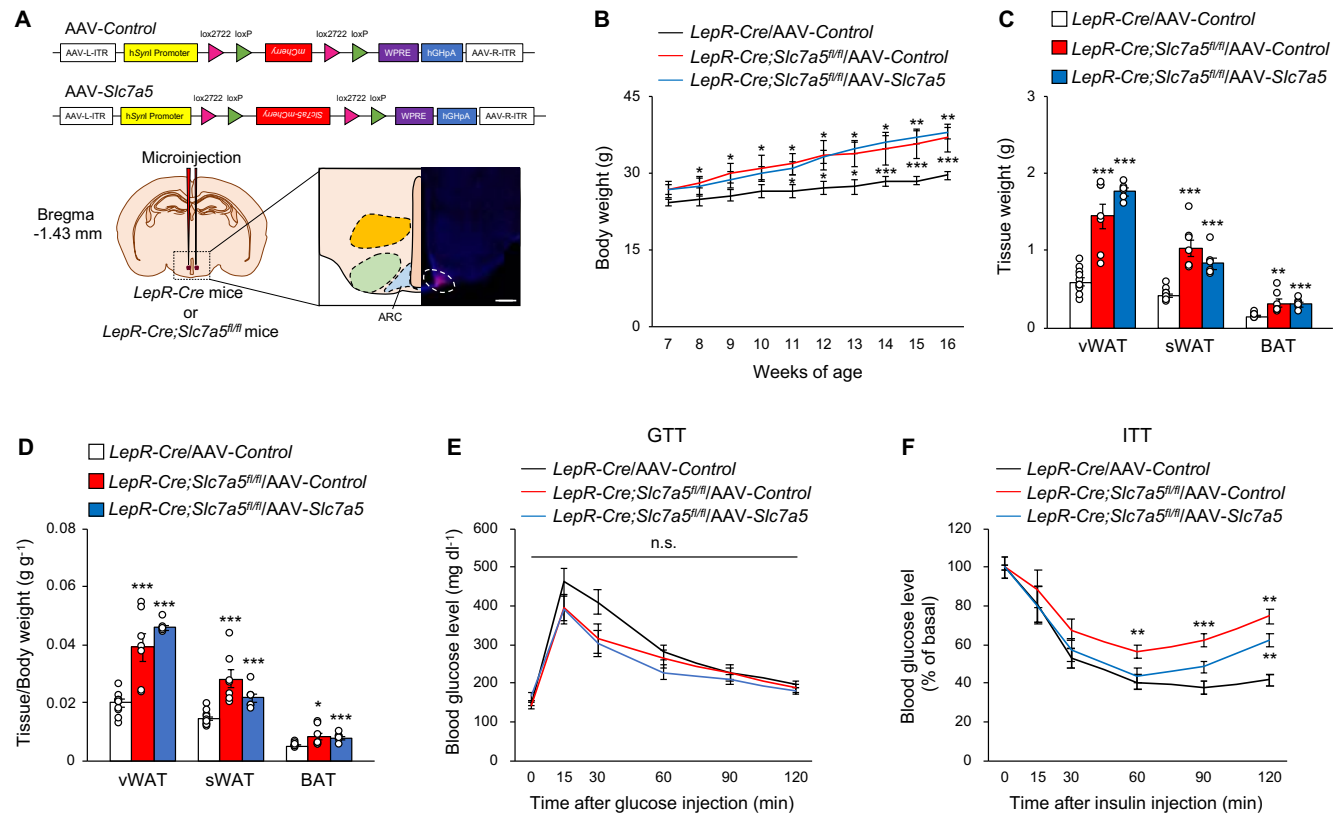
Supplemental Figure. 4 HFD-induced obesity is exacerbated in *LepR-Cre;Slc7a5^{fl/fl}* mice.

(**A**) Weekly body weight is shown for *LepR-Cre;Slc7a5^{fl/fl}* mice and control mice fed a HFD (n = 5 or 8, *P < 0.05, two-way ANOVA with Bonferroni *post hoc* test). (**B** and **C**) Adipose tissue weights (**B**) and adipose tissue weights normalized to body weight (**C**) are shown for *LepR-Cre;Slc7a5^{fl/fl}* mice and control mice at 16 weeks of age (n = 5 or 8, *P < 0.05, **P < 0.01, ***P < 0.001, two-tailed Student's *t*-test). (**D**) GTTs were performed in *LepR-Cre;Slc7a5^{fl/fl}* mice and control mice after a 6 hr fast at 16 weeks of age (n = 6, *P < 0.05, **P < 0.01). (**E**) ITTs were performed in *LepR-Cre;Slc7a5^{fl/fl}* mice and control mice after a 6 hr fast at 16 weeks of age (n = 6, *P < 0.05, **P < 0.01, two-way ANOVA with Bonferroni *post hoc* test). All of the mice used in this study were male.

A

µCT analysis

Slc7a5^{fl/fl}   *LepR-Cre;Slc7a5^{fl/fl}*

B

□ *Slc7a5^{fl/fl}*
■ *LepR-Cre; Slc7a5^{fl/fl}*

n.s.

BV/TV (%)

C

µCT analysis

WT   *LepR-Cre*

D

□ WT
■ *LepR-Cre*

n.s.

BV/TV (%)

Supplemental Figure. 5 Analysis of bone volume in vertebrae from *LepR-Cre;Slc7a5^{fl/fl}* mice and femurs from *LepR-Cre* mice.

(**A**) µCT analysis, scale bar, 1 mm and (**B**) BV/TV ratio as determined by µCT of vertebrae from *LepR-Cre;Slc7a5^{fl/fl}* mice at 14 weeks of age ($n = 7$ or 8, two-tailed Student's *t*-test). (**C**) µCT analysis, scale bar, 1 mm, and (**D**) BV/TV ratio as determined by µCT of femurs from *LepR-Cre* mice and control mice at 12-16 weeks of age ($n = 4$ or 6, two-tailed Student's *t*-test). All of the mice used in this study were male.

Supplemental Figure. 6 LepR-expressing ARC neurons do not contribute to LAT1-dependent regulation of systemic energy and bone homeostasis.

(**A**) Schematic diagram of the bilateral viral microinjection into the ARC, and representative validation image of mCherry expression in the ARC. Scale bar, 500 μm. (**B**) Weekly body weight after injection of AAV-*Control* or AAV-*Slc7a5* into the ARC is shown for *LepR-Cre;Slc7a5^fl/fl* mice and control mice (*n* = 6 to 11, **P* < 0.05: versus *LepR-Cre*/AAV-*Control*, two-way ANOVA with Bonferroni *post hoc* test). (**C** and **D**) Adipose tissue weights (**C**) and adipose tissue weights normalized to body weight (**D**) are shown for *LepR-Cre;Slc7a5^fl/fl* mice and control mice injected with AAV-*Control* or AAV-*Slc7a5* into the ARC at 16 weeks of age (*n* = 6 to 11, **P* < 0.05, ***P* < 0.01, ****P* < 0.001, two-tailed Student's *t*-test with Bonferroni correction). (**E**) GTTs were performed in *LepR-Cre;Slc7a5^fl/fl* mice and control mice after a 6 hr fast at 16 weeks of age (*n* = 6 to 11, two-way ANOVA with Bonferroni *post hoc* test). (**F**) ITTs were performed in *LepR-Cre;Slc7a5^fl/fl* mice and control mice injected with AAV-*Control* or AAV-*Slc7a5* into the ARC after a 6 hr fast at 16 weeks of age (*n* = 6 to 11, ***P* < 0.01, ****P* < 0.001: versus *LepR-Cre*/AAV-*Control*, two-way ANOVA with Bonferroni *post hoc* test). All of the mice used in this study were male.
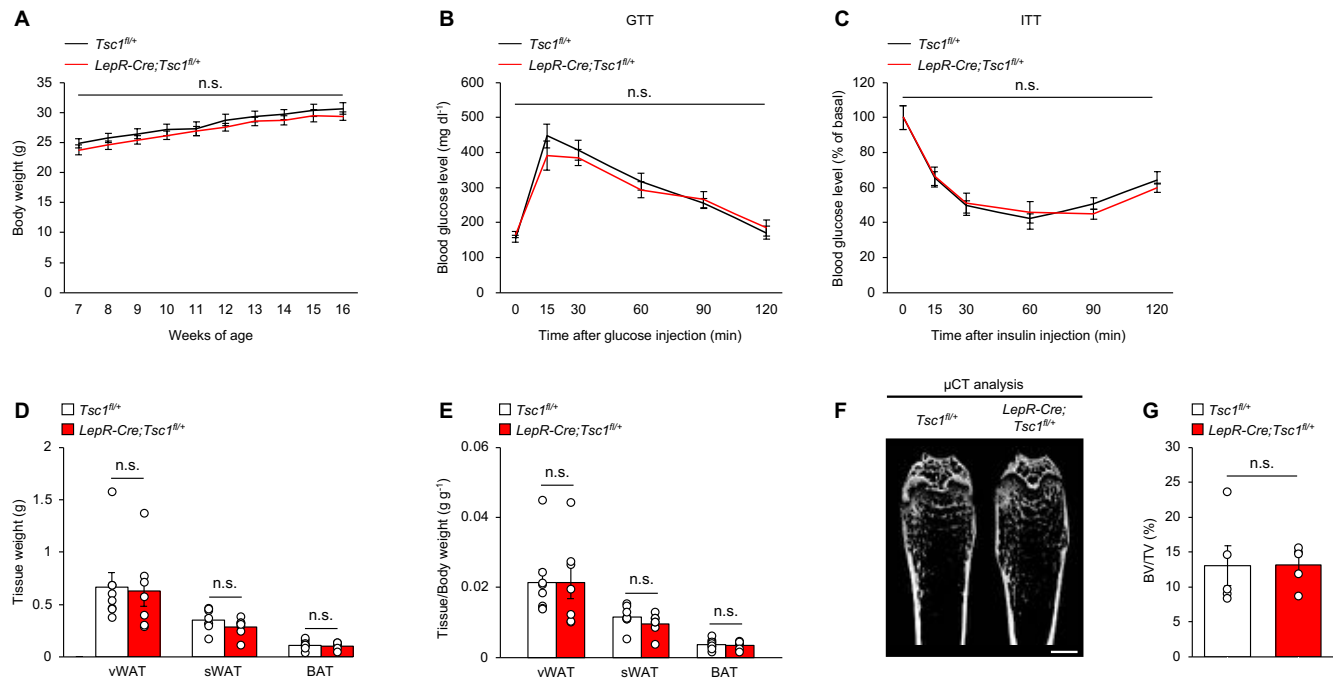
Supplemental Figure. 7 *LepR-Cre;Tsc1^{fl/+}* mice does not display any abnormal energy homeostasis.

(**A**) Weekly body weight is shown for *LepR-Cre;Tsc1^{fl/+}* mice and control mice fed a NC (n = 7 or 8, two-way ANOVA with Bonferroni *post hoc* test). (**B**) GTTs were performed in *LepR-Cre;Tsc1^{fl/+}* mice and control mice after a 6 hr fast at 16 weeks of age (n = 7 or 8, two-way ANOVA with Bonferroni *post hoc* test). (**C**) ITTs were performed in *LepR-Cre;Tsc1^{fl/+}* mice and control mice after a 6 hr fast at 16 weeks of age (n = 7 or 8, two-way ANOVA with Bonferroni *post hoc* test). (**D** and **E**) Adipose tissue weights (**D**) and adipose tissue weights normalized to body weight (**E**) are shown for *LepR-Cre;Tsc1^{fl/+}* mice and control mice at 16 weeks of age (n = 7 or 8, two-tailed Student's *t*-test). (**F**) μCT analysis, scale bar, 1 mm, and (**G**) BV/TV ratio as determined by μCT of femurs from *LepR-Cre;Tsc1^{fl/+}* mice and control mice at 12-16 weeks of age (n = 5, two-tailed Student's *t*-test). All of the mice used in this study were male.